Scientific paper

Green Biosynthesis of Spherical Silver Nanoparticles by Using Date Palm (*Phoenix Dactylifera*) Fruit Extract and Study of Their Antibacterial and Catalytic Activities

Saeed Farhadi,[1,*] Bahram Ajerloo[1] and Abdelnassar Mohammadi[2]

[1] *Department of Chemistry, Lorestan University, Khoramabad 68151-44316, Iran*

[2] *Department of Biology, Lorestan University, Khoramabad 68151-44316, Iran*

** Corresponding author: E-mail: sfarhadi1348@yahoo.com*
Tel.: +98-6633120618, fax: +98-6633120611

Received: 30-09-2016

Abstract

In this work, we have synthesized spherical silver nanoparticles (Ag NPs) by a low-cost, rapid, simple and ecofriendly approach using Date palm fruit extract as a novel natural reducing and stabilizing agent. The product was characterized by UV-visible spectroscopy, X-ray diffraction (XRD), Fourier transform infrared spectroscopy (FTIR), field emission scanning electron microscopy (FESEM), transmission electron microscopy (TEM), atomic force microscopy (AFM), energy-dispersive X-ray (EDX) spectroscopy and Zeta potential measurements. The reaction conditions including time, content of reducing agent and silver nitrate, temperature and pH were investigated. The optimum yield of Ag NPs was obtained when 10 mM of silver nitrate was reacted with Date fruit extract at pH 11 and heated it to 55 °C within 10 minutes. The elemental and crystalline nature of Ag NPs were confirmed from EDX and XRD analysis. SEM and TEM images showed that the Ag NPs were spherical and with sizes in the range of 25–60 nm. On the base of FT-IR analysis, it can be stated that the functional groups present in bio-molecules of Date fruits are responsible for the reduction and stabilization of Ag NPs, respectively. The Ag NPs showed good antibacterial activity against a few human pathogenic bacteria. The catalytic activity of the Ag NPs for rapid and efficient reduction of toxic nitro compounds into less toxic corresponding amines by using $NaBH_4$ was also investigated.

Keywords: Biosynthesis, Silver nanoparticles, Date palm fruit extract, Antibacterial activity, Nitro reduction, Catalyst

1. Introduction

Among various transition metal nanoparticles, silver nanoparticles (Ag NPs) have attracted considerable attention in nanoscience and nanotechnology due to their excellent optical and electronic properties as well as their wide applications in various fields such as catalysis,[1] surface enhanced Raman scattering,[2] degradation of environmental pollutants,[3] biosensors[4] cancer therapy5 and antibacterial effects.[6] Several synthetic strategies have been developed for the synthesis of Ag NPs including photochemical,[7] sonochemical,[8] sovothermal[9] and spin coating methods.[10] Among these, chemical reduction of a silver ions (Ag^+) in presence of a stabilizer is the most frequently applied method for the preparation of Ag NPs as stable colloidal dispersions in water or organic solvents.[11] The major drawback of chemical method is that the highly reactive chemical reductants as well as the stabilizers such as synthetic polymers, surfactants and dendrimers used in this method cause chemical toxicity and serious environmental problems, thus limiting their utility.

In recent years, biosynthesis of metal nanoparticles has received considerable attention due to the growing need to develop clean and nontoxic chemicals, environmentally friendly solvents and renewable materials.[12] The selection of a non-toxic reducing agent, a cost-effective and easily renewable stabilizing agent and an environmentally benign solvent system are the three main criteria for a greener metal nanoparticles synthesis. In this regard, a great deal of effort has been devoted toward the biosynthesis of silver nanoparticles using bacteria,[13–17] fungi,[18-20] actinomycetes,[21–23] yeast[24] and viruses[25–27] but the rate of nanoparticle synthesis is faster using fruits and plants extracts than microbes, and the pro-

duced nanoparticles are more stable.[28] In recent regards, the synthesis of Ag NPs has been reported by using the natural extract of leaves, seeds and or roots of plants such as *Nelumbo nucifera*,[29] *Anisochilus carnosus,* [30] *Mimusops elengi*,[31] *marine macroalga Chaetomorpha linum*,[32] *Bunium persicum*,[33] *Olea europaea,*[34] *Hamamelis virginiana,*[35] *Justicia adhatoda*,[36] *Suaeda acuminata*,[37] *Mentha piperita*,[38] *Phlomis*,[39] *Pennyroyal,*[40] *Murraya keenigii*,[41] *Mangifera indica*,[42] *Nicotiana tobaccum*,[43] *Bunium persicum,*[44] *Hamamelis virginiana*.[45] However, the reaction time of Ag^+ ions for complete reduction in these works was very long. To enable the biosynthesis methods of Ag NPs to compete with the chemical methods, there is a need to achieve faster synthesis rates with high monodispersion. The use of fruit extracts of plants is an appropriate candidate for this purposes. Several papers on the synthesis of Ag NPs using the extract of fruits such as *Terminalia chebula,*[46] *Solanum trilobatum*,[47] *Dillenia indica,*[48] *Solanum lycopersicums,*[49] *Tanacetum vulgare,*[50] *Crataegus douglasii,*[51] *Emblica Officinalis,*[52] and *Kiwifruit* [53] have been reported in the literatures.

The Date palm tree *(Phoenix dactylifera),* a tropical and subtropical tree, is one of mankind's oldest cultivated plants, and it has played an important role in the day-to-day life of the people for the last 7000 years.[54] Dates are produced in 35 countries worldwide and cultivated on about 2.9 million acres of land. The world production of date fruit estimate to be more than 7000000 metric tons, and Iran (14% of world production) is the second major producer after Egypt (17% of world production). Figure 1 shows the photographs of Date palm trees ant their fruits. The Date fruit is considered to be an inexpensive and easily available important fruit in Iran.[55] The Date palm fruits are an important source of nutrition, especially in the arid regions where due to the extreme conditions, very few plants can grow. Date fruit also shows some functional properties in the food industry, such as water-holding, oil-holding, emulsifying and gel formation. Indeed, Date fruit can be incorporated in food products to modify textural properties, avoid synthesis and stabilize high fat food and emulsions.[56] The study by Abdelhak has shown that different varieties of ripe Date fruits contained mainly p-coumaric, ferulic and sinapic acids and some cinnamic acid derivatives.[57] The in vitro study by Vayalil reported that the aqueous extract of Date fruits has antioxidative and antimutagenic properties.[58] On the other hand, the study by Bilgari had shown

Figure 1(a)-(d) Photographs of Date palm trees and their fruits.

a strong correlation between the antioxidant activity and the total phenolic and total flavonoids of palm dates.[59] The Date fruit is rich in phytochemicals like carbohydrates and sugars, phenolics, sterols, carotenoids, anthocyanins, procyanidins, and flavonoids.[60] Most of the biomolecules can act as reducing and capping agent in the reactions. Then, the Date fruits extract that are inherently rich in these phytochemicals could be used as a novel reducing agent for synthesizing Ag NPs in large-scale production.

In this paper, we report on rapid, simple and low-cost synthesis of Ag NPs by the reduction of aqueous Ag^+ solution using Date fruit extract. To our knowledge, this is the first report on the use of Date fruit for the rapid synthesis of Ag NPs. The nearly monodisperse Ag were formed under mild conditions, without any additive protecting nanoparticles. The formation of Ag NPs was recorded by the UV-visible spectra. Additionally, the obtained Ag NPs were analyzed by Fourier transform infrared (FT-IR) spectra, and X-ray diffraction (XRD), scanning electron microscopy (SEM), transmission electron microscopy (TEM), and energy-dispersive X-ray (EDX) spectroscopy. The rapid approach using Date fruit extract would be suitable for developing a biological process for large-scale production. Various parameters (e.g. concentration of the reactants, reaction temperature, pH and time) were optimized that would increase the yield of nanoparticle synthesis. The antibacterial and catalytic activities of the biologically synthesized Ag NPs were also investigated.

2. Experimental

2. 1. Materials

Silver nitrate ($AgNO_3$), $NaBH_4$, 4-nitrophenol, and 4-nitroanilin were obtained from Merck and were of analytical grade. Double distilled de-ionized water was used for the experiments. All glass wares were properly washed with distilled water and dried in oven.

2. 2. Preparation of Date Palm Fruit Extract

Date Palm fruit extract was used as a reducing and stabilizing agent for the synthesis of Ag NPs. Date palm fruits were purchased from local supermarket in Iran and used for the synthesis of silver nanoparticles. The fresh fruits of Date washed repeatedly with distilled water to remove the dust and organic impurities present in it. About 15 g of fruit were crushed into fine pieces with sterilized knife. The fruit of Date Palm were taken into the 250 ml beaker containing 100 mL double distilled de-ionized water and then the solution was stirred for 30 min and filtered through Whatman No.1 filter paper twice. The obtained light yellow extract was stored in refrigerator at 4 °C. The extract is used as reducing agent as well as stabilizing agent.

2. 3. Synthesis of Ag Nanoparticles

In a typical experiment, Ag NPs were prepared by using Date fruit extract as follows: in a 50 mL round-bottom flask equipped with a magnet bar, 3 ml of aqueous solution of Date fruit extract was mixed with 20 ml of 10 mM aqueous silver nitrate solution. The mixture was then heated at 55 °C under constant stirring for an appropriate time (e.g. 10 min) in an oil bath. The formation process and the optical properties of the silver nanoparticles were identified from both the color change and UV-Vis spectra of the solution**.** In order to remove the Ag NPs product, the solution was centrifuged at 5500 rpm for 20 min. The supernatant was decanted and the precipitate was re-dispersed in double distilled water for another round of centrifugation. The precipitate was then washed with deionized water for three times to remove any impurities if any. Finally, the washed precipitate was dried in an oven maintained at 60 °C for 2 h and finally ground into powder for characterization.

In a similar manner described above, a series of experiments were conducted to investigate the effect of various parameters including reaction time, Ag^+ ion concentration, the Date fruit extract amount, pH and temperature on the reaction. The reaction mixtures were monitored by a UV-Vis spectrophotometer at different time intervals and the Ag NPs were characterized further. The effect of pH on the Ag NPs synthesis was determined by adjusting the pH of the reaction mixtures (10 mM silver nitrate, 3 mL date extract) to 3, 5, 7, 9, 11 or 13 by using 0.1 M HCl or NaOH aqueous solutions. The effect of the silver salt was determined by varying the concentration of silver nitrate (0.1, 1, 10 and 100 mM). The Date fruit extract content was varied to 1, 3, 5, 7, 9 mL, while keeping the silver nitrate concentration at a level of 10 mM. To study the effect of temperature on nanoparticle synthesis, reaction mixtures containing 3 mL Date extract, and 10 mM $AgNO_3$ at pH 11 were incubated at 25, 40, 55 or 70 °C.

2. 4. Methods of Characterization

The UV-visible absorption spectra of Ag NPs colloidal solutions were recorded on a double beam UV-visible spectrometer (Cary 100, VARIAN) operated at a resolution of 2 nm with quartz cells with path length of 1 cm in 300–800 nm range. Blanks were prepared with deionized (DI) water. Infrared spectra were obtained using a FT-IR 160 Schimadzu Fourier transform infrared spectrophotometer using KBr pellets. The XRD pattern of the silver nanoparticles was obtained on an X-ray diffractomer (PANalytical/X'Pert Pro MPD) using Cu Kα (1.54059 Å) radiation. The particle size and shape was confirmed using a scanning electron microscope (MIRA3 TESCAN) equipped with EDX attachment. Transmission electron microscopy (TEM) observations were conducted on a Philips CM120 microscope at the accelerating voltage of 200 kV. AFM images were recorded on a multi-mode ato-

mic force microscopy (ARA-AFM, model Full Plus, ARA Research Co., Iran). The surface charge of samples was measured with Zeta potential measurements in water (NICOMP 380ZLS Zeta potential/Particle sizer). Magnetic measurements were carried out at room temperature using a vibrating sample magnetometer (VSM, Magnetic Daneshpajoh Kashan Co., Iran) with a maximum magnetic field of 10 kOe.

2. 5. Antibacterial Tests

Antibacterial activity of the biosynthesized Ag NPs was evaluated against strains of Gram-positive bacteria: Bacillus cereus (PTCC 1015), Staphylococcus aureus (1431) and Staphylococcus epidermidis (PTCC 1114), Gram–negative bacteria: Escherichia coli (PTCC 1330) and Klebsiella pneumonia (PTCC 1290) by modified Kirby-Bauer disk diffusion method [66]. Bacteria were cultured for 18 h at 37 °C in Nutrient agar medium and then adjusted with sterile saline to a concentration of 2×10^6 cfu/mL. Bacterial suspension in Petri dishes (8 cm) containing sterile Mueller-Hinton agar (MA) were cultured using a sterile cotton swab. The compounds were dissolved in water and sterile paper discs of 6 mm thickness were saturated with 30 µl of silver nanoparticles and then placed onto agar plates which had previously been inoculated with the tested microorganisms. Amikacin (30 µg/disk) for gram negative and penicillin for gram positive (10 µg/disk) was used as positive controls. After incubation at 37 °C for 24 h, the diameter of inhibition zone was measured. The diameter of such zones of inhibition was measured using a meter ruler, and the mean value for each organism was recorded and expressed in millimetres.

2. 6. Catalytic Tests

In order to study the catalytic performance of the biosynthesized Ag NPs, the reduction of 4-nitrophenol (4-NP) to 4-amiophenol (4-AP) by excess sodium borohydride ($NaBH_4$) in aqueous solution was used as the model reaction. In a typical catalytic reaction, 3 mL of aqueous solution of 4-NP (0.1 mM) and 0.5 mL of aqueous $NaBH_4$ (10 mM) solution were mixed together in a standard quartz cell, having 1 cm path length and then 1 mL of aqueous Ag suspensions (0.5 mg mL^{-1}) was added to the reaction mixture under constant magnetic stirring. Immediately after that, the solution was transferred to a standard quartz cell, and the concentration of p-nitrophenol in the reaction mixture was monitored by the UV-visible absorption spectra recorded with a time interval of 2 min in a scanning range of 200–800 nm at ambient temperature. For recycling experiment, after completion of the reaction the catalyst was recovered by centrifugation. The precipitate was washed repeatedly with deionized water in consecutive washing cycles. Ultrasonic treatment was used in every cycle in order to re-disperse the catalyst and remove adsorbed impurities. After washing, the catalyst was used directly for recycling test. After each recycle, the centrifuge supernatant was collected and detected by Atomic absorption spectroscopy to determine the content of Ag metal. The reduction 4-nitroaniline was also investigated under the same conditions.

3. Results and Discussion

3. 1. Phytoreduction of Silver Ions

A study on phytosynthesis of Ag NPs by the aqueous fruit extract of date was carried out in this work. During the visual observation, silver nitrate treated with date fruit extract showed a color change from yellow to brown within 20 min whereas no color change could be observed in silver nitrate solution without date extract (Figure 2). The appearance of yellowish brown color in fruit extract treated flask is a clear indication for the formation of Ag NPs. This color arises due to excitation of surface plasmon resonance (SPR) vibrations in Ag nanoparticles.

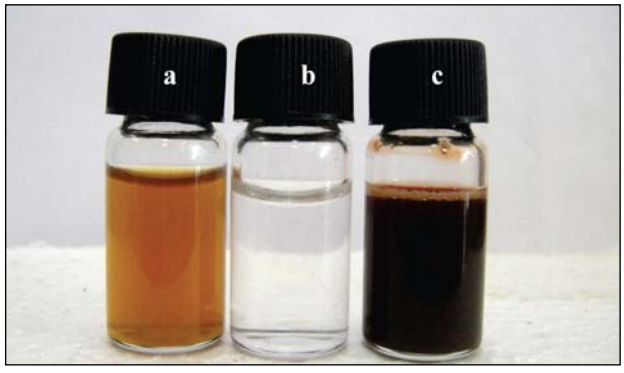

Figure 2. Photographs of: (a) aqueous extract of date fruits, (b) 10 mM of aqueous $AgNO_3$ solutions, and (c) Colloidal aqueous Ag NPs solution formed by reduction of $AgNO_3$ with Date fruit extract.

3. 2. UV–Visible Absorption Studies

UV–Vis spectroscopy is a powerful tool to study the formation of Ag NPs. The reaction mixtures containing silver salt and Date fruit extract were, therefore characterized by UV–Visible spectroscopy. Based on UV–Vis spectroscopy various chemical and physico-parameters (concentration of the fruit extract and silver salt, pH, temperature and reaction time) were optimized for the reduction Ag+ ions to Ag NPs using Date fruit extract.

To optimize the reaction time, a time variation study was carried out using the concentration of $AgNO_3$ (10 mM) and aqueous date extract (3 mL). Figure 3(a) shows the UV–Vis absorption spectra of Ag NPs synthesized at

different time durations. It is observed that the intensity of SPR bands increases as the reaction time progresses and within 10 min a considerable intensity of the SPR bands is achieved. However, these values were hardly changed after 10 min. It suggested that the reduction time of Ag^+ was almost completed within 10 min in the presence of date extract. Therefore, the optimal reaction time for the reduction Ag^+ ions to Ag NPs using Date fruit extract is 10 min. As shown in the inset of Fig. 3(a), after the reaction between Ag^+ and date extract, the color was changed from clear yellow to dark brown and it shows the formation of Ag NPs.

Next, various concentrations of silver nitrate solution (0.1–100 mM) were reacted with 3 mL fruit extract. Figure 3(b), shows the UV–Vis absorption spectra of Ag NPs obtained at different concentrations of $AgNO_3$ (0.1, 1, 10 and 100 mM). At 0.1 mM concentration, an observable SPR band was not appeared, indicating very low yield of Ag NPs formed (Figure 3(b), curve i), but with increasing concentration of $AgNO_3$ to 1 mM, the SPR of Ag NPs appears at 395 nm and remarkably increases with the increase of $AgNO_3$ concentration to 10 mM with increasing in the peak wavelength to 410 nm (Figure 3(b), curves i and ii, respectively). High intensity of the 410 nm SPR band indicates increasing concentration of nanoparticle. However, further increasing the concentration of $AgNO_3$ from 10 to 100 mM did not increase the SPR band further–in contrast, it give a broad SPR band with decreased intensity and shifted to longer wavelength region (~425 nm). This phenomenon may be due to the fast growth of the particles at high concentration. The appearance of red shifted band at higher concentration of $AgNO_3$ suggests the formation of larger particles. The yield of Ag NPs increased with the increase in silver nitrate concentration (0.1–10 mM) and maximum yield was obtained with 10 mM, and this concentration was selected for further studies.

Additionally, the effect of the date extract amount on the synthesis of Ag NPs was investigated under the provided reaction conditions, and the results are shown in Figure 3(c). As observed, with increasing the date extract quantity from 1 to 3 mL in 20 mL of 10 mM Ag^+ ion solution, the intensity of characteristic SPR absorption bands for Ag NPs increases (Figure 3(c), curves i and ii) and then decreases when the date extract increases further (Figure 3(c), curves iii-v). The maximum absorption was found at a concentration of 3 mL fruit extract. From the UV-Vis absorption spectrum in Figure 3(c), it was observed that there is a shift in wavelength from 400 to 412 nm indicating a redshift with increase in date extract concentration from 1 to 3 mL. Accordingly, it can be concluded that with the increase in Date extract amount, the size of Ag nanoparticles increases.

The temperature also affected the process of silver reduction. The effect of reaction temperature was also evaluated with varying reaction temperatures from 25 to 75 °C (Figure 3(d)). As shown in Figure 3(d) (curves i and ii), the reaction mixtures incubated at room temperature (25 °C) and 40 °C showed less pronounced SPR peaks during a long time of 50 min while by heating the reaction mixtures at 55 and 70 °C the reduction process was faster and the intense peaks were developed within a short time of 10 min (Figure 3(d), curves iii and iv). This indicates that higher temperature facilitates the formation of Ag NPs due to the increase in the reaction rate. The maximum SPR peak intensity was detected at 70 °C. However, a slight increase in SPR band intensity occurs at 75 °C when compared with the temperature of 55 °C. Then, the temperature of 55 °C is preferred for further study. It is noteworthy to mention that with the increase in reaction temperature, UV-Vis spectra show sharp narrow peaks at lower wavelength regions (~412 nm at 55 and 70 °C), which indicate the formation of smaller nanoparticles, whereas, at lower reaction temperature, the peaks observed at higher wavelength region (425 nm at 25 °C) which clearly indicates increase in silver nanoparticles size. It is a well-known fact that when the temperature is increased, the reactants are consumed rapidly leading to the formation of smaller nanoparticles [61, 62].

Among the various parameters, the initial pH of solution plays a significant role in the synthesis of metal nanoparticle. Thus, in the present study, the effect of pH on the synthesis of Ag NPs was studied at acidic, natural and basic values using 3 ml Date fruit extract and 10 mM $AgNO_3$. As can be seen in Figure 3(e) (curves i and ii) the formation of Ag nanoparticles was not observed at all at acidic pHs 3 and 5. Under the acidic conditions, biomolecules are likely to be inactivated. This suggests that acidic pH is not favorable for the Ag NPs synthesis. At pH 7, the Ag NPs formation was observed at relatively low concentration, as confirmed by the appearance of a weak absorbance band at about 425 nm (Figure 3(e), curve iii). However, Ag NPs were readily obtained at pH higher than 7, as evidenced through progressive evolution of the characteristic SPR band in the spectral region from 400 to 415 nm. As can be seen in Figure 3(e) (curves iv-vi), the intensity of the SPR band of these Ag NPs increased significantly upon increasing the pH to 9, 11 and then 13, indicating that correspondingly higher yields of Ag NPs were obtained, probably due to the presence of a considerable number of reactive functional groups to bind with silver ions. In addition, a slight red shift of the SPR band of the Ag NPs (from 400 to 415 nm) occurred upon increasing the pH. These results suggest that larger-diameter Ag NPs were obtained at higher pHs. The optimal pH for nanoparticle synthesis was chosen to be pH 11, which is in good agreement with the reported literature.[63] The differences in the amount of Ag NPs obtained over the range of pH could be ascribed to a variation in the dissociation constants (pKa) of functional groups (OH and COOH) on the biomolecules that are involved.[64]

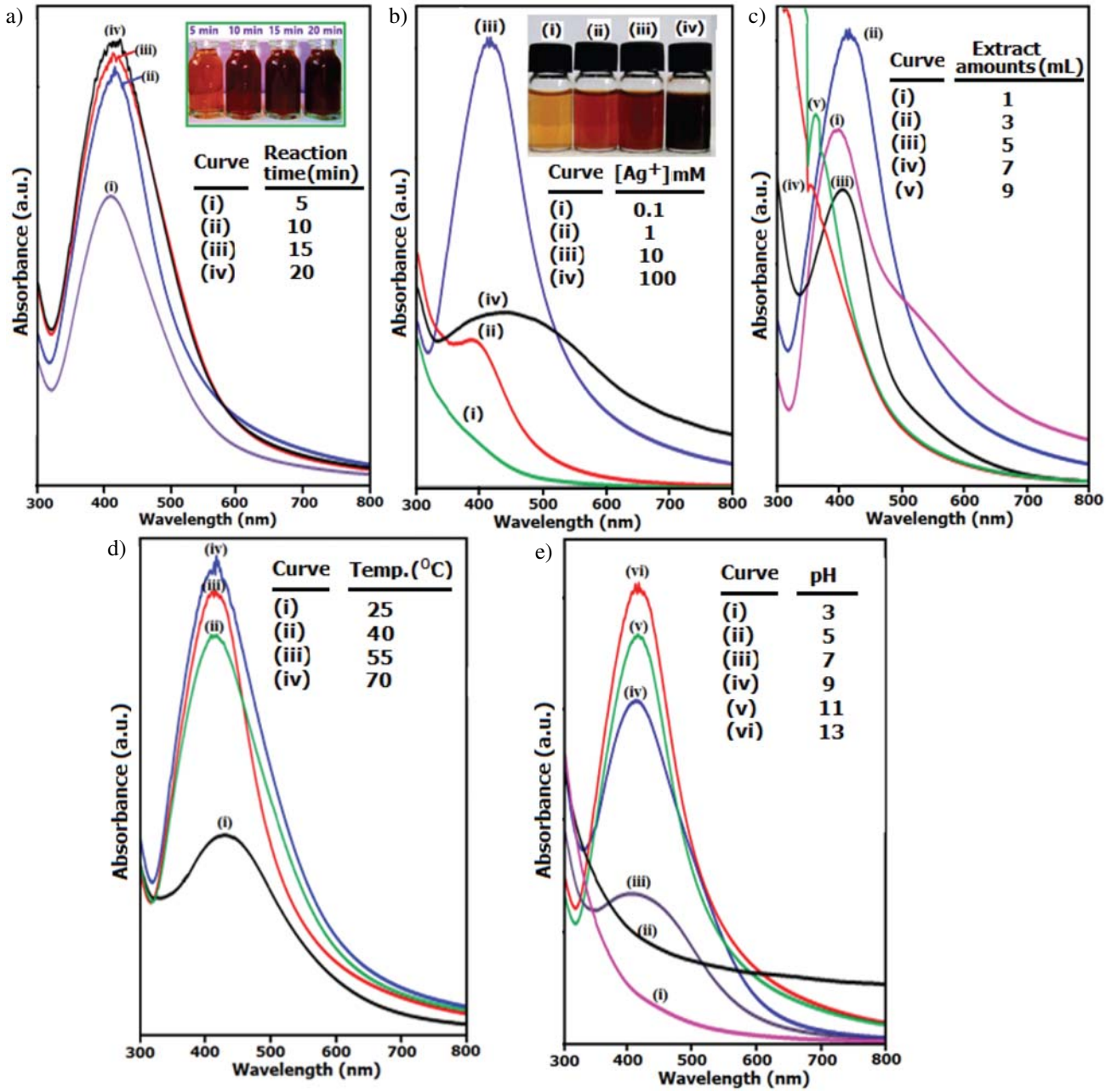

Figure 3. Effect of various parameters on the synthesis of Ag NPs: (a) The effect of reaction time; The inset photo shows the color change of solution with time of reaction, (b) The effect of Ag+ Concentration; The inset photo shows the color change of solution at different concentrations of $AgNO_3$, (c) The effect of different amounts of Date fruit extract, (d) the effect of different temperatures and (e) the effect of pH.

3. 3. XRD Analysis

Figure 4 shows the XRD pattern of Ag NPs synthesized using Date fruit extract after the complete reduction of Ag^+ to Ag under the optimized conditions (10 mM $AgNO_3$, 3 mL Date extract, pH 11 at 55 °C for 10 min). As observed in the XRD pattern, the four characteristic diffraction peaks at 2θ values of 38.10°, 44.15°, 64.67°, and 77.54° can be indexed to the (111), (200), (220), and (311) reflection planes of faced center cubic (fcc) structure of silver (JCPDS card no 04.0784). The considerable broadening of the diffraction peaks demonstrates the nanometer nature of the Ag particles. The average crystallite size of the Ag product is approximately 39.5 nm as estimated by the Debye–Scherrer equation: $D_{XRD} = 0.9\lambda/(\beta\cos\theta)$, where D_{XRD} is the average crystallite size, λ is the wavelength of Cu Kα radiation, β is the corrected full-width at half-maximum of the main diffraction peak of (111), and θ is the Bragg angle. The XRD pattern obtained is consistent with earlier reports.[65,66]

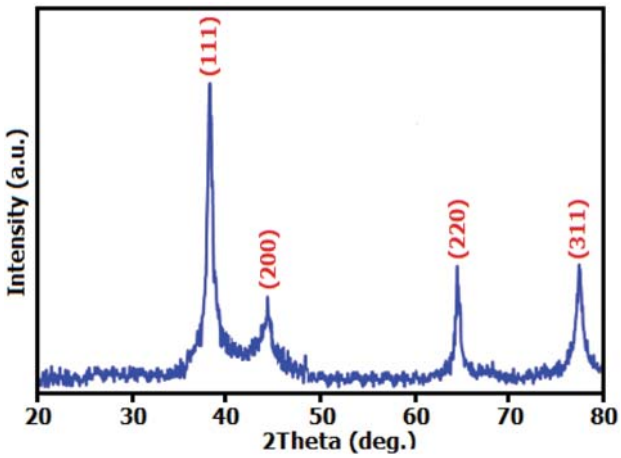

Figure 4. XRD pattern of Ag NPs synthesized by Date fruit extract.

3. 4. SEM, TEM and EDX Analysis

The size and morphology of the Ag NPs were determined via SEM, TEM and AFM images. Figure 5 shows the SEM images of the as-prepared Ag NPs. From the SEM images in different magnifications (Figure 5(a)–(c)), it is clearly evident that the product consists of extremely fine particles with sphere-like morphologies that appreciably aggregated as clusters due to the extremely small dimensions and high surface energy of the obtained nanoparticles. We also can find from the images that the morphology of the particles is almost homogeneous. The resulting images show the presence of large number of spherical nanoparticles with an average particle size of 42.5 nm. The EDX was used to further characterize the composition of the sample. Figure 5(d) shows the EDX spectrum of the Ag NPs prepared by using Date

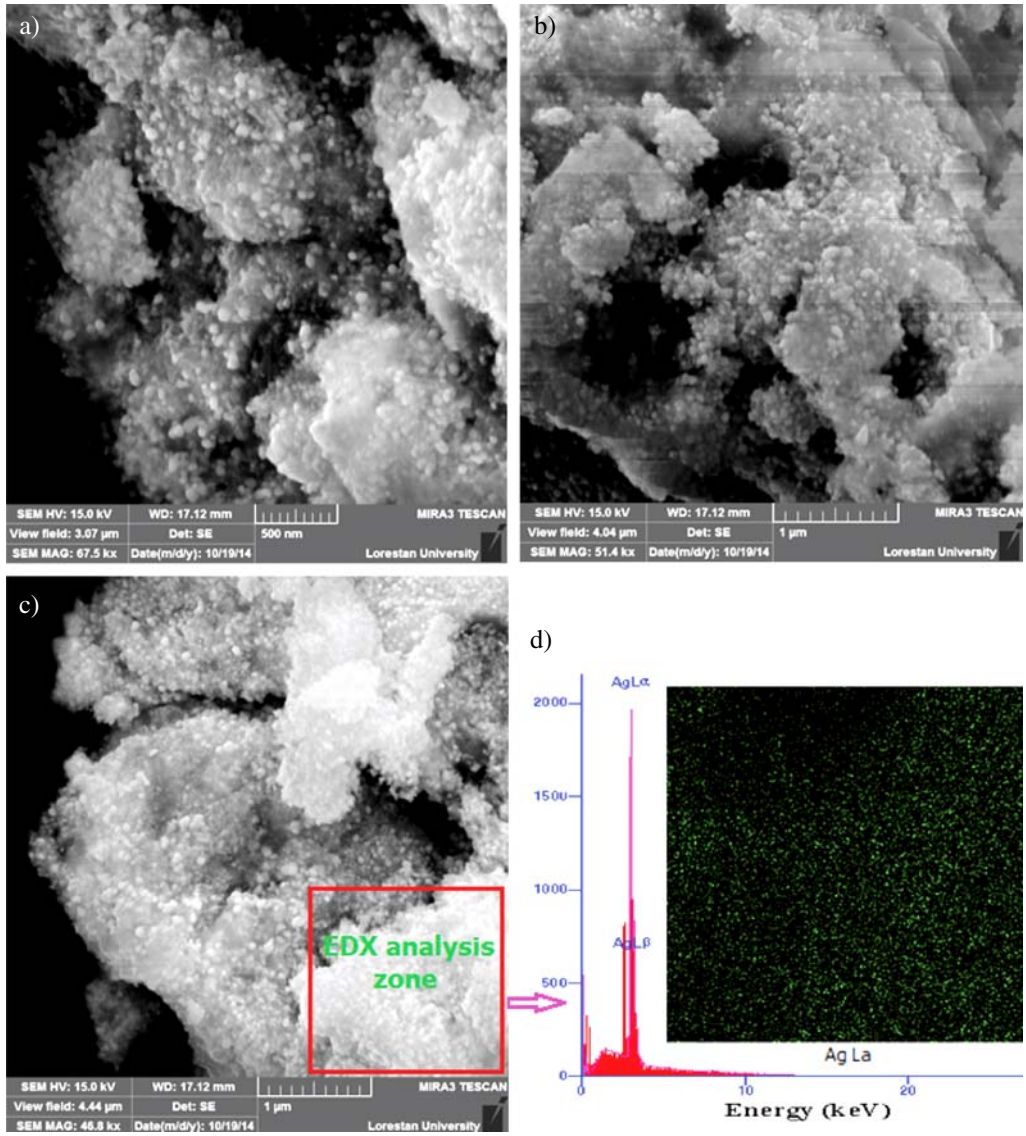

Figure 5. (a–c) SEM images of the as-prepared Ag NPs, (d) EDX elemental spectrum of the Ag NPs. The inset of Figure 5(d) shows EDX elemental mapping for Ag NPs.

fruit extract as reducing agent. The intense peaks around 3.40 keV and 3.45 keV are correspond to the binding energies of Ag $K_{L\alpha}$ and Ag $K_{L\beta}$, respectively, while the peaks situated blow 0.5 keV corresponding of N, C and O from Date fruit extract. Further, the EDX elemental mapping of the product in the inset of Figure 5(d) displays the uniform distribution of the Ag element. The results further indicate that the Ag NPs have been successfully prepared in this work.

The TEM image and size distribution of the Ag NPs are shown in Figure 6. The TEM sample was prepared by dispersing the powder in ethanol by ultrasonic vibration. It can be seen from Figure 6 that the nanoparticles show approximately sphere-like morphologies with a uniform size. Because of the small dimensions and high surface energy of the particles, it is easy for them to aggregate. We also can find from this figure that the morphology of the particles is almost homogeneous. To investigate the size distribution of the Ag NPs, the particle size histogram was also determined from the TEM image. The inset of Figure 6 shows the size distribution of the Ag particles. It is clear that the diameter sizes of the Ag NPs are in the range of 25 to 60 nm with a narrow size distribution. The average particle size is approximately 40 nm, which is in agreement with the result calculated for the half-width of diffraction peaks using the Scherrer's formula, allowing for experimental error.

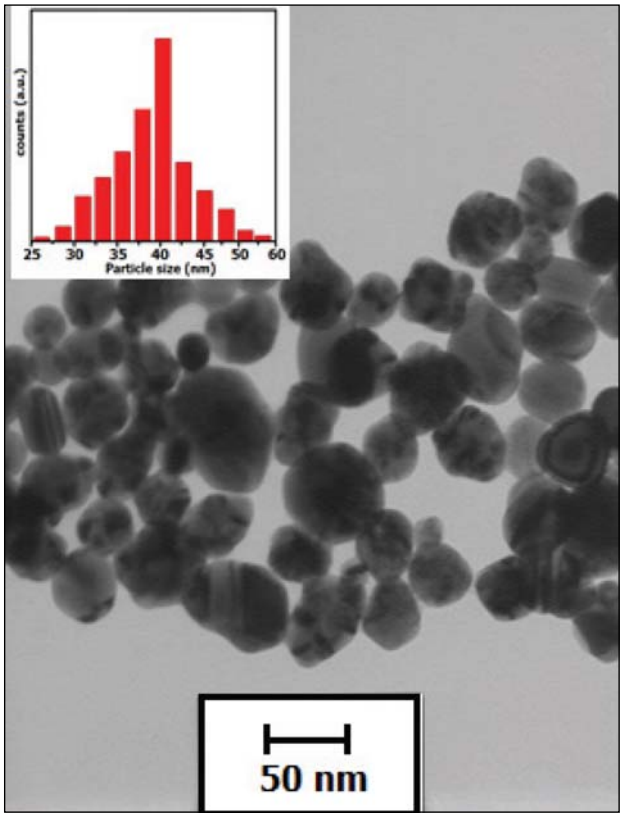

Figure 6. TEM image of the Ag NPs. The inset shows the size distribution of the Ag NPs.

AFM is a beneficial tool for studying various morphological features and parameters. Since, it has the advantage of probing in deep insights of surface topography qualitatively due to its both lateral and vertical nanometer scale spatial resolution. The AFM images in Figure 7 display the surface morphology of the Ag-NPs formed by Date fruit extract. As observed in Figure 7(a), AFM image reveals the appearance of spherical nanoparticles and their respective particle size and morphology clearly were close to those determined by the SEM and TEM images. As can be seen from Figure 7(b), the surface of Ag NPs sho-

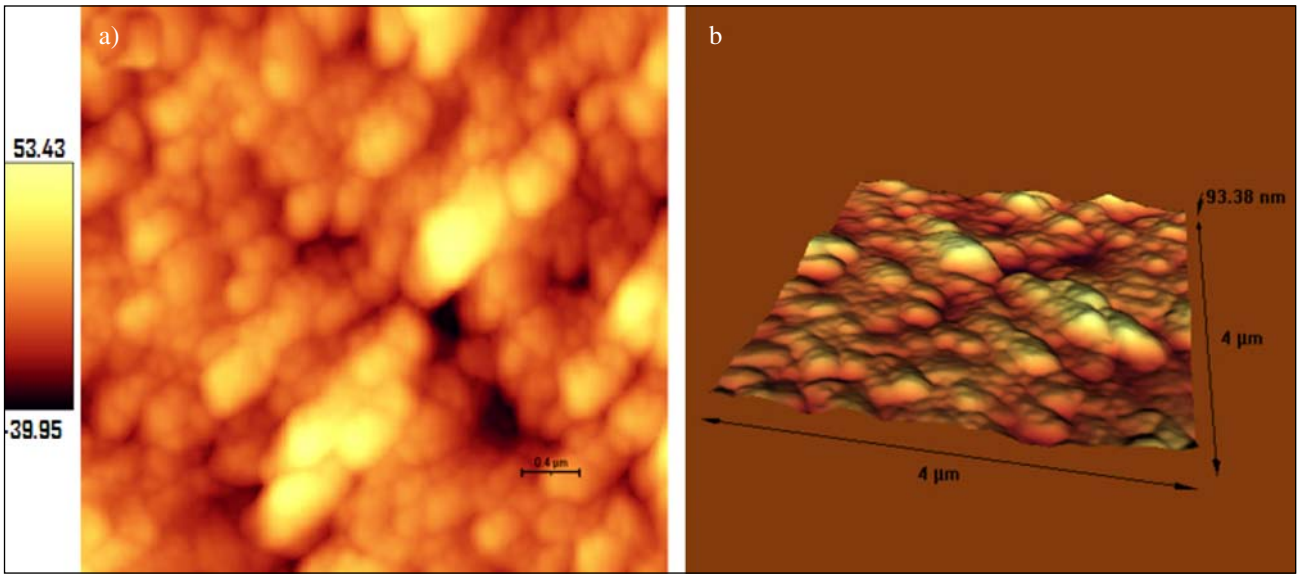

Figure 7. (a) and (b) AFM images of the Ag NPs.

wed a dense and uniform packed structure. Thus, the Ag NPs could provide a biocompatible and rough surface for biological uses, e.g., cell immobilization.

3. 5. Zeta Potential Measurements

Zeta potential provides the information about the stability of nanoparticles and surface charge. Zeta potential is an essential parameter for characterization of stability in aqueous colloidal Ag-NPs suspensions. Zeta potential of the synthesized Ag NPs is pictured in Figure 8. The zeta potential value was measured to be about –35 mV which confirms the good stability of the colloidal Ag NPs aqueous suspension formed by reduction of $AgNO_3$ with Date fruit extract.[67] The high negative values illustrate the repulsion between the particles and thereby attainment of better stability of Ag NPs formation avoiding agglomeration in aqueous solutions.

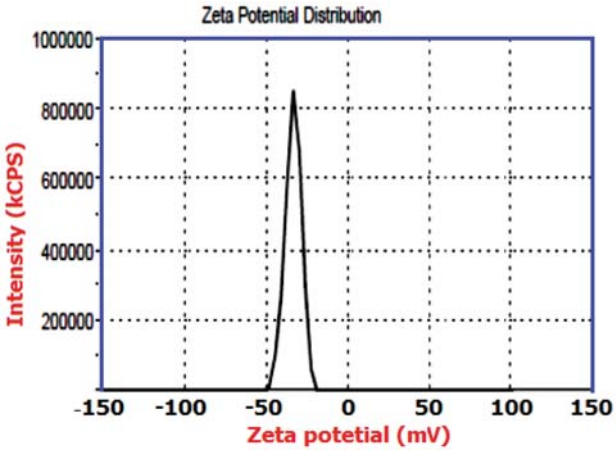

Figure 8. Zeta potential analysis of colloidal Ag NPs solution prepared with Date fruit extract.

3. 6. FT-IR Chemical Analysis

The identification of the possible biomolecules responsible for the reduction and the stabilization of biosynthesized Ag NPs can be achieved by the FTIR studies. It has been reported that the Date palm fruit is rich in phytochemicals like carbohydrates (mainly glucose, sucrose and fructose), phenolic acids, sterols, carotenoids, anthocyanins, procyanidins and flavonoids.[60] Figure 9(A) shows the structures of some phytochemicals present in Date fruits As can be seen, these components are containing carboxyl (–COOH), phenolic –OH and carbonyl (C=O) functional groups. Figure 9(B) shows FT-IR spectra recorded for the Date fruit extract and the Ag NPs synthesized with the Date extract before and after washing. The FT-IR spectrum of Date extract in Figure 9(B) (spectrum a) shows phenolic O–H, C=O, and

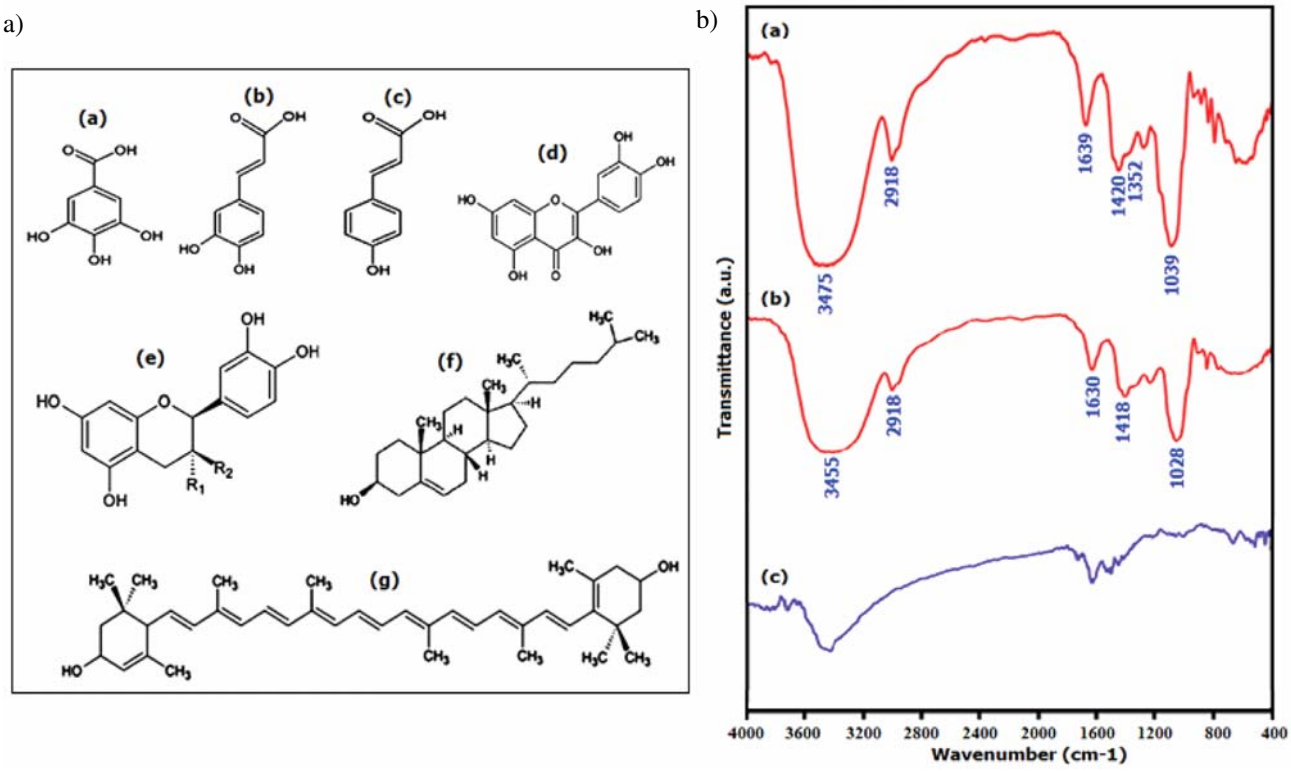

Figure 9. (A) The structure of some of phytochemicals present in Date fruits: (a)-(c) Phenolic acids, (d) a Flavonoid, (e) a Procyanidin, (f) a Sterol, (g) a Carotenoid. (B) FT-IR spectra of: (a) Date palm fruit extract, (b) Ag NPs capped with Date fruit extract solution and (c) Ag NPs after washing with deionized water

C–OH stretching bands, corresponding to a number of bands at 3475, 1639, and 1039 cm^{-1}, respectively. The absorption bands at 2918, 1420, and 1352 cm^{-1} are related to the C–H stretching bands in Date fruit. As shown in Figure 9(B), (spectrum b), after the reduction of $AgNO_3$ the decreases in intensity of bands at 3450 and 1039 cm^{-1} and redshift of these bands signify the involvement of the OH groups in the reduction process. On the hand the shift of the band from 1639 cm^{-1} to 1630 cm^{-1} is attributed to the binding of C=O groups with Ag NPs. On the base of FT-IR analysis, it can be stated that the hydroxyl, carboxyl and carbonyl functional groups present in carbohydrates, flavonoids, tannins and phenolic acids of Date fruit extract may be accountable for the reduction of the Ag^+ ions and stabilization of Ag NPs. In an experiment, the Ag NPs capped with Date extract were washed with deionized water for three times and the FT-IR spectrum of the dried precipitate was again taken for the purity of the sample. As can be clearly seen in Figure 9(B), (spectrum c), the intensity of the characteristic bands of biomolecules markedly decreases after washing the product, confirming the removal of biomolecules on the surface of Ag NPs.

From the FTIR analysis and previously reported mechanisms,[68–70] it can be stated that the hydroxyl and carbonyl groups present in carbohydrates, flavonoids, procyanidin and phenolic compounds are powerful reducing agents and they may be accountable for the bioreduction of Ag^+ ions leading to Ag^0 nanoparticle synthesis. FTIR study confirms that the carbonyl groups of biomolecules have a strong ability to bind metal ions and they may be encapsulated around the Ag NPs forming a protective coat-like membrane to avoid the agglomeration and thus results in nanoparticle stabilization in the medium. Thus, the Date fruit extract components act as bioreductants and surfactants too. The plausible mechanism of the formation of Ag NPs by using a Flavonoid biomolecule as a typical reducing agent is shown in Figure 10. In this pursuit, proteins and all secondary metabolites of extract play a critical role in both reducing and capping mechanism for nanoparticle formation.

3. 7. Antibacterial Activity of Ag Nanoparticles

The antibacterial activity of Ag NPs were analyzed against five bacteria: Bacillus cereus, Staphylococcus aureus, Staphylococcus epidermidis, Klebsiella pneumonia, and Escherichia coli by disk diffusion method. The results of the antibacterial activity of silver nanoparticles were showed in Figure 11. The Figure shows that Ag NPs have good antibacterial activity; bacteria cells have been killed at the concentration of 30 µg/ml. Table 1 represented the inhibition zone of these bacteria. Highest activity of Ag NPs was obtained against epidermidis, while lowest activity were observed against B. cereus and E. coli. Biosynthesized Ag NPs exhibit more antimicrobial activity on

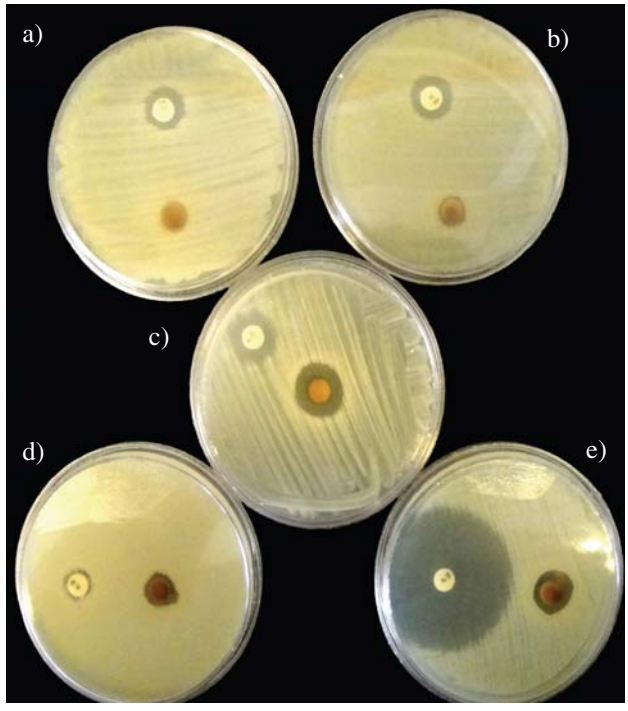

Figure 11. Images of antibacterial activities of Discs 30 µg/mL Ag NPs on (a) E. Coli, (b) K. Pneumonia, (c) S. Epidermidis, (d) B. Cereus. (e) S. Aureus.

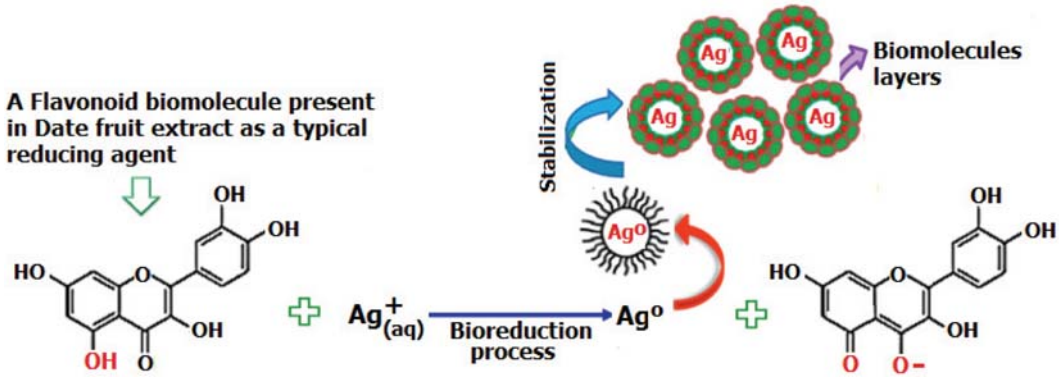

Figure 10. The plausible mechanism of the formation of Ag NPs using Date fruit extract

Table 1. Average of inhibition zones synthesized silver nanoparticles with Date fruit extract.

Entry	Bacteria	Type	Inhibition zone diameter (mm)	
			Silver nanoparticle	Disc standard
1	E. Coli	Gram-negative	11	13
2	K. Pneumonia	Gram-negative	11	13
3	S. Epidermidis	Gram-positive	17	14
4	B. Cereus	Gram-positive	12	11
5	S. Aureus	Gram-positive	13	41

gram-positive microorganism than gram-negative. The potential antimicrobial activities showed by Ag NPs have made them encouraging candidates as novel generation antimicrobials.

3. 8. Catalytic Activity of Ag Nanoparticles

To evaluate the catalytic activity of the Ag NPs prepared in this work by using Date fruit extract, the reduction of 4-nitrophenol (4-NP) and 4-nitroaniline (4-NA) in aqueous solution by excess $NaBH_4$ was used as the model systems. The catalytic process was monitored by UV–Vis spectroscopy as shown in Figure 12. From Figure 12(a), it was seen that an absorption peak of 4-NP undergoes a red shift from 317 to 400 nm immediately upon the addition of aqueous solution of $NaBH_4$, corresponding to a significant change in solution color from light yellow to yellow-green due to formation of 4-nitrophenolate ion. In the absence of Ag NPs catalyst (0.5 mg), the absorption peak at 400 nm remained unaltered for a long duration, indicating that the $NaBH_4$ itself cannot reduce 4-nitrophenolate ion without a catalyst. In the presence of Ag NPs catalyst and $NaBH_4$ the 4-NP was reduced, and the intensity of the absorption peak at 400 nm decreased gradually with time and after about 24 min it fully disappeared (Figure 12(a)). In the meantime, a new absorption peak appeared at about 295 nm and increased progressively in intensity. This new peak is attributed to the typical absorption of 4-aminophenol (4-AP). This result suggests that the catalytic reduction of 4-NP exclusively yielded 4-AP, without any other side products. In the reduction process, the overall concentration of $NaBH_4$ was 10 mM and 4-NP was 0.1 mM. Considering the much higher concentration of $NaBH_4$ compared to that of 4-NP, it is reasonable to assume that the concentration of BH_4^- remains constant during the reaction. In this context, pseudo-first-order kinetics could be used to evaluate the kinetic reaction rate of the current catalytic reaction, together with the UV–Vis absorption data in Figure 12(a). The absorbance of 4-NP is proportional to its concentration in solution; the absorbance at time t (A_t) and time t = 0 (A_0) are equivalent to the concentration at time t (C_t) and time t = 0 (C_0). The rate constant (k) could be determined from the linear plot of $\ln(C_t/C_0)$ versus reduction time in minutes. As expected, a good linear correlation of $\ln(C_t/C_0)$ versus time was obtained as shown in the inset of Figure 12(a), whereby a kinetic reaction rate constant k is estimated to be 1.34×10^{-1} min^{-1}. Figure 12(b) shows the UV-Vis absorption spectra of the reduction of 4-nitroaniline by $NaBH_4$ at various reaction times in the presence of Ag NPs. The observed peak at 385 nm for the 4-nitroaniline shows a gradual decrease in intensity with time and a new peak appeared at 295 nm indicating the formation of p-phenylenediamine (1,4-PD). As shown in Figure 12(b), it took 24 min for the complete reduction of 4-NA in the presence of Ag NPs (0.5 mg).

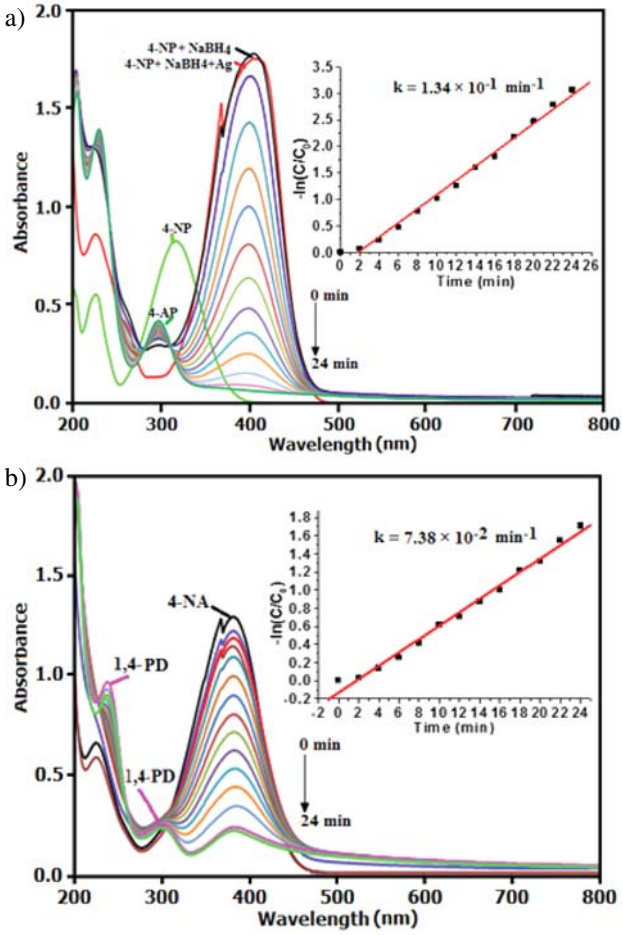

Figure 12. UV–Vis spectra of (a) 0.1 mM 4-nitrophenol (4-NP) with 10 mM NaBH4 and (b) 0.1 mM 4-nitroaniline (4-NA) with 10 mM NaBH4 in the presence of Ag NPs as catalyst. The insets show the plots of $\ln(C_t/C_0)$ against the reaction time for pseudo-first-order reduction kinetics of 4-NP and 4-NA in the presence of excess $NaBH_4$ (10 mM) in aqueous solutions.

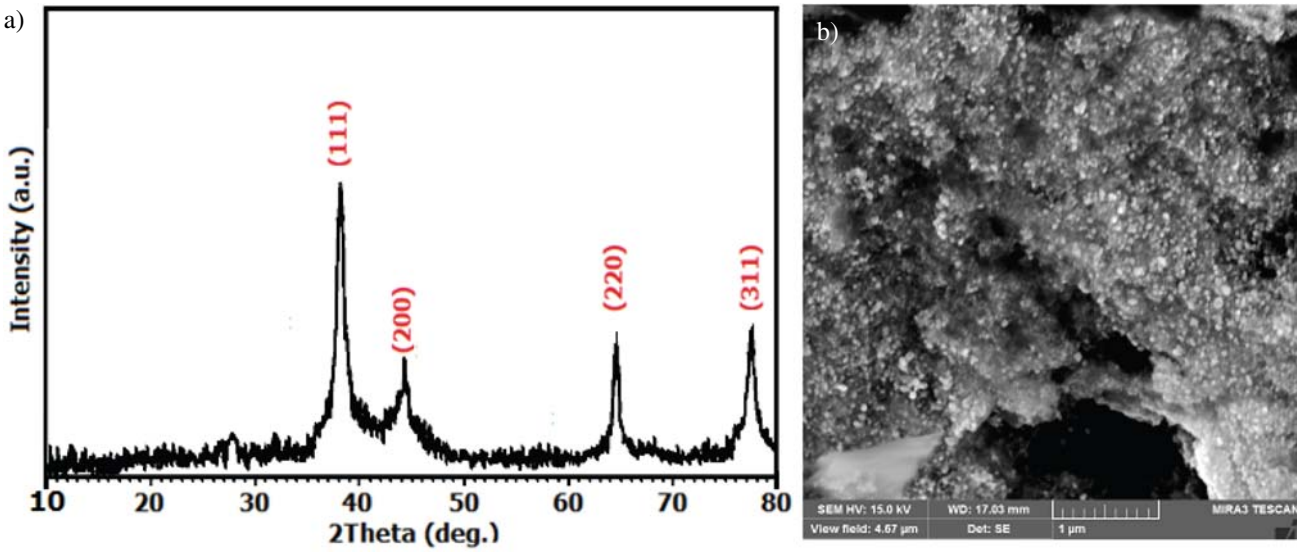

Fig. 13. (a) XRD pattern and (b) SEM image of the recovered Ag NPs after the fourth cycle.

The corresponding k value was 7.38×10^{-2} min^{-1} (see the inset in Figure 12(b)). The results indicated that Ag NPs exhibited considerably high activity for the reduction of nitroarenes with $NaBH_4$ as the hydrogen donor.

The reusability of catalysts is a very important parameter to assess the catalyst practicability. Therefore, the recovery and reusability of the Ag catalyst was investigated for the reduction of 4-NP under the present reaction conditions. After the completion of reaction, Ag NPs were separated from the reaction mixture by centrifugation. The catalyst was washed with water and ethanol several times, dried and employed for the next reaction. The activity of the four consecutive runs (98, 98, 97 and 95%) revealed the practical recyclability of the applied catalyst. No significant loss in activity was observed for up to four catalytic cycles, thereby indicating that the as-prepared catalyst is stable and efficient in the reduction of nitro-compounds. As shown in Fig. 13(a) and (b), XRD and SEM image of the recycled catalyst did not show significant change after the fourth run in comparison with the fresh catalyst (see Figures 4 and 5). This observation confirmed that the Ag NPs are stable under the reaction conditions and are not affected by the reactants.

Moreover, we have compared the obtained results in the reduction of 4-NP with $NaBH_4$ catalyzed by Ag NPs prepared in this work with some reported catalysts in the literature (Table 2). It is clear that with respect to the reaction conditions and/or reaction times, the present method

Table 2. Comparison of the result obtained for the reduction of 4-NP in the present work with those obtained by some reported catalysts.

Entry	Catalyst	Conditions	Time	Ref.
1	Ni-PVA/SBA-15	H_2O, $NaBH_4$, r.t.	85 min	**[71]**
2	Hierarchical Au/CuO NPs	H_2O, $NaBH_4$, r.t	80 min	**[72]**
3	Cu NPs	THF/H_2O, $NaBH_4$, 50 °C	2 h	**[73]**
4	PdCu/graphene	EtOH/H_2O, $NaBH_4$, 50 °C	1.5 h	**[74]**
5	Au-GO	H_2O, $NaBH_4$, r.t.	30 min	**[75]**
6	$CoFe_2O_4$ NPs	H_2O, $NaBH_4$, r.t.	50 min	**[76]**
7	$FeNi_2$ nano-alloy	H_2O, $NaBH_4$, r.t	60 min	**[77]**
8	$NiCo_2$ nano-alloy	H_2O, $NaBH_4$, r.t.	30 min	**[78]**
9	CdS/GO	H_2O, $NaBH_4$, r.t.	30 min	**[79]**
10	dumbbell-like CuO NPs	H_2O, $NaBH_4$, r.t.	32 min	**[80]**
11	Ni NPs	H_2O, $NaBH_4$, r.t.	16 min	**[81]**
12	$CuFe_2O_4$ NPs	H_2O, $NaBH_4$, r.t.	14 min	**[82]**
13	Au NPs	H_2O, $NaBH_4$, r.t.	4 min	**[83]**
14	Pd/RGO/Fe_3O_4 NPs	H_2O, $NaBH_4$, r.t.	1 min	**[84]**
15	Cu/Fe_3O_4 NPs	H_2O, $NaBH_4$, r.t.	55 sec	**[85]**
16	Cu NPs/perlite	H_2O, $NaBH_4$, r.t.	**2.5 min**	**[86]**
17	**Ag NPs**	**H_2O, $NaBH_4$, r.t.**	**24 min**	**This work**

is more suitable and/or superior (Table 2, entries 1–10). It is clear that reaction in the presence of most reported catalysts required longer reaction times. However, compared with some these reports, the present catalyst also presented close or lower catalytic activity for the reduction of 4-NP (Table 2, entries 11–16). Furthermore, compared with the other catalysts, the Ag NPs can be easily prepared using Date fruit extract without the use of harsh, toxic and expensive chemicals which is very important in practical applications.

4. Conclusions

In the present work, Date fruit extract was used as an effective reducing as well as capping agent for the biosynthesis Ag NPs in aqueous solution. The synthesis of Ag NPs was affected by the variation in reaction conditions such as time, temperature, concentration of extract and silver solution and pH. The synthesized Ag NPs were spherical, 25–60 nm in size, crystal in nature and showed absorption spectrum at ~400–420 nm. The formed Ag NPs were quite stable, showed good antimicrobial activity and were utilized as a catalyst for the reduction of several aromatic nitro-compounds into their corresponding amino derivatives. Thus Date extract can be effectively used for the synthesis of Ag NPs. Further experiments for the synthesis other metal nanoparticles such as Au, Pd, and Cu, using Date fruit extract are in progress in our laboratory. Synthesis of metallic nanoparticles using green resources like Date fruit extract is a challenging alternative to chemical synthesis, since this novel green synthesis is cost effective, pollutant free and eco-friendly synthetic route.

5. Acknowledgements

The authors gratefully acknowledge the Lorestan University Research Council and Iran Nanotechnology Initiative Council (INIC) for their financial supports.

6. References

1. K. Nishioka, T. Sueto, N. Saito, *Appl. Surf. Sci*. **2009**, *255*, 9504–9507. https://doi.org/10.1016/j.apsusc.2009.07.079
2. Y. W. C. Cao, R. C. Jin, C. A. Mirkin, *Sci.* **2002**, *297*, 1536–1540. https://doi.org/10.1126/science.297.5586.1536
3. V. K. Vidhu, D. Philip, *Micron* **2014**, *56*, 54–62. https://doi.org/10.1016/j.micron.2013.10.006
4. C. J. Kirubaharan, D. Kalpana, Y. S. Lee, A. R. Kim, D. J. Yoo, K. S. Nahm, G. G. Kumar, *Ind. Eng. Chem. Res*., **2012**, *51*, 7441–7446. https://doi.org/10.1021/ie3003232
5. M. Rahban, A. Divsalar, A. A. Saboury, A. Golestani, *J. Am. Phys. Chem*. C **2010**, *114*, 5798–5803.
6. M. Miranzadeh, M. Z. Kassaee, L. Sadeghi, M, Sadroddini, M. Razzaghi-Kashani, N. Khoramabadi, *Nanochem. Res.* **2016**, *1*, 1–8.
7. M. Ohtaki, N. Toshima, *Chem. Lett*. **1990**, *4*, 489–492. https://doi.org/10.1246/cl.1990.489
8. Y. Mizukoshi, K. Okisu, Y. Maeda, T. A. Yamamoto, R. Oshima, Y. Nagata, *J. Am. Phys. Chem. B* **1997**, *101*, 7033–7037. https://doi.org/10.1021/jp9638090
9. M. Khademalrasool, M. Farbod, *J. Nanostruct.* **2015,** *5*, 415–422
10. S. Darvishi, S. M. Borghei, S. A. Hashemizadeh, *J. Nanostruct.* **2012,** *2*, 501–504.
11. B. J. Wiley, Y. Sun, Y. Xia, *Acc. Chem. Res.* **2007**, *40*, 1067–1076. https://doi.org/10.1021/ar7000974
12. H. Ahmad, K. Rajagopal, A.H. Shah, *Int. J. Nano Dimens.* **2016**, *7*, 97–108.
13. T. Klaus, R. Joerger, E. Olsson, C. G. Granqvist, *Proc. Natl. Acad. Sci.* **1999***, 96*, 13611–13614. https://doi.org/10.1073/pnas.96.24.13611
14. Y. Roh, R. J. Lauf, A. D. McMillan, C. Zhang, C. J. Rawn, J. Bai, T. J. Phelps, *Solid State Commun.* **2001**, *118*, 529–534. https://doi.org/10.1016/S0038-1098(01)00146-6
15. B. Nair, T. Pradeep, *Cryst. Growth. Des.* **2002**, *2*, 293–298. https://doi.org/10.1021/cg0255164
16. P. Yong, N. A. Rowson, J. P. G. Farr, I. R. Harris, L. E. Macaskie, *Biotechnol. Bioeng.* **2002***, 80*, 369–379. https://doi.org/10.1002/bit.10369
17. M. I. Husseiny, M. A. El-Aziz, Y. Badr, M. A. Mahmoud, *Spectrochim. Acta A* **2007***, 67*, 1003–1006. https://doi.org/10.1016/j.saa.2006.09.028
18. P. Mukherjee, A. Ahmad, D. Mandal, S. Senapati, S. R. Sainkar, M. I. Khan, R. Parishcha, P. V. Ajaykumar, M. Alam, R. Kumar, M. Sastry, *Nano. Lett.* **2001**, *1*, 515–519. https://doi.org/10.1021/nl0155274
19. P. Mukherjee, A. Ahmad, D. Mandal, S. Senapati, S. R. Sainkar, M. I. Khan, R. Ramani, R. Parischa, P. A. Ajaykumar, M. Alam, M. Sastry, R. Kumar, *Angew. Chem. Int. Ed.* **2001***, 40*, 3585–3588. https://doi.org/10.1002/1521-3773(20011001)40:19<3585::AID-ANIE3585>3.0.CO;2-K
20. A. Ahmad, S. Senapati, M. I. Khan, R. Kumar, *J. Biomed. Nanotechnol.* **2005**, *1*, 47–53. https://doi.org/10.1166/jbn.2005.012
21. A. Ahmad, S. Senapati, M. I. Khan, R. Kumar, R. Ramani, V. Srinivas, M. Sastry, *Nanotechnology* **2003**, *14*, 824–828. https://doi.org/10.1088/0957-4484/14/7/323
22. A. Ahmad, S. Senapati, M. I. Khan, R. Kumar, M. Sastry, *Langmuir* **2003**, *19*, 3550–3553. https://doi.org/10.1021/la026772l
23. M. Sastry, A. Ahmad, M. I. Khan, R. Kumar, *Curr. Sci*. **2003**, *85*, 162–170.
24. M. Kowshik, S. Arhtaputre, S. Kharrazi, W. Vogel, J. Urban, S. K. Kulkarni, K. M. Paknikar, *Nanotechnology* **2003**, *14*, 95–100. https://doi.org/10.1088/0957-4484/14/1/321
25. W. Shenton, T. Douglas, M. Young, G. Stubbs, S. Mann, *Adv. Mater.* **1999**, *11*, 253–256.

https://doi.org/10.1002/(SICI)1521-4095(199903)11:3<253::AID-ADMA253>3.0.CO;2-7
26. S. W. Lee, C. Mao, C. Flynn, A. M. Belcher, *Sci.* **2002**, *296*, 892–895. https://doi.org/10.1126/science.1068054
27. A. Merzlyak, S. W. Lee, *Curr. Opin. Chem. Biol.* **2006**, *10*, 246–252. https://doi.org/10.1016/j.cbpa.2006.04.008
28. S. M. Ali, V. Anuradha, N. Yogananth, R. Rajathilagam, A. Chanthuru, S. M. Marzook, *Int. J. Nano Dimens.* **2015**, *6*, 197–204.
29. N. T. M. Tho, T. N. M. An, M. D. Tri, T. V. M. Sreekanth, J.-S. Lee, P. C. Nagajyothi, K. D. Lee, *Acta Chim. Slov.* **2013,** *60,* 673–678.
30. P. P. Vijaya., M. S. Ali, R. S. Saranya, N. Yogananth, V. Anuratha, P. K. Parveen, *Int. J. Nano Dimens.* **2013**, *3*, 255–262.
31. P. Prakash, P. Gnanaprakasam, R. Emmanuel, S. Arokiyaraj, M. Saravanan, *Colloids Surf. B* **2013**, *108*, 255–259. https://doi.org/10.1016/j.colsurfb.2013.03.017
32. R. R. R. Kannan, R. Arumugam, D. Ramya, K. Manivannan, P. Anantharaman, *Appl. Nanosci.* **2013**, *3*, 229–233. https://doi.org/10.1007/s13204-012-0125-5
33. A. Rostami-Vartooni, M. Nasrollahzadeh, M. Alizadeh, *J. Colloid Interface Sci.* **2016**, *470*, 268–275. https://doi.org/10.1016/j.jcis.2016.02.060
34. B. Sadeghi, *Int. J. Nano Dimens.* **2014**, *5*, 575–581.
35. A. Rostami-Vartooni, M. Nasrollahzadeh, M. Alizadeh, J. Alloys Compd. **2016,** *680,* 309–314. https://doi.org/10.1016/j.jallcom.2016.04.008
36. K. M. Ponvel, T. Narayanaraja, J. Prabakaran, *Int. J. Nano Dimens.* **2015**, *6*, 339–349.
37. H. R. Rajabi, H. Deris, H. S. Faraji, *Nanochem. Res.* **2016**, *1*, 177–182.
38. D. M. Ali, N. Thajuddin, K. Jeganathan, M. Gunasekhran, *Colloids Surf. B* **2011**, *85*, 360–365. https://doi.org/10.1016/j.colsurfb.2011.03.009
39. A. R. Allafchian, S. Z. Mirahmadi-Zare, S. A. H. Jalali, S. S. Hashemi, M. R. Vahabi, *J. Nanostruct Chem.* **2016**, *6*, 129–135.
40. S. Sedaghat, A. Esmaeili-Agbolag, S. bagheriyan, *J. Nanostruct Chem.* **2016**, *6*, 25–27. https://doi.org/10.1007/s40097-015-0176-8
41. D. Philip, C. Unni, S. A. Aromal, V. K. Vidhu, *Spectrochim. Acta A* **2011**, *78*, 899–904. https://doi.org/10.1016/j.saa.2010.12.060
42. D. Phillip, *Spectrochim. Acta A* **2011**, *78*, 327–331. https://doi.org/10.1016/j.saa.2010.10.015
43. K. S. Prasad, D. Pathak, A. Patel, P. Dalwadi, R. Prasad, P. Patel, K. Selvaraj, *J. Afr. Biotechnol.* **2011**, *10*, 8122–8130. https://doi.org/10.5897/AJB11.394
44. M. L. Rao, N. Savithramma, *J. Pharm. Sci. Res.* **2011**, *3*, 1117–1121.
45. K. Satyavani, T. Ramanathan, S. Gurudeekan, *Dig. J. Nanomater. Biostruct*. **2011**, *6*, 1019–1024.
46. T. J. I. Edison, M. G. Sethuraman, *Process. Biochem.* **2012**, *47*, 1351–1357. https://doi.org/10.1016/j.procbio.2012.04.025
47. M. Ramar, B. Manikandan, P. N. Marimuthu, T. Raman, A. Mahalingam, P. Subramanian, S. Karthick, A. Munusamy, *Spectrochim. Acta A* **2015**, *140*, 223–228. https://doi.org/10.1016/j.saa.2014.12.060
48. S. Singha, J. P. Saikia, A. K. Buragohain, *Colloids Surf. B* **2013**, *102*, 83–85. https://doi.org/10.1016/j.colsurfb.2012.08.012
49. M. Umadevi, M. R. Bindhu, V. Sathe, *J. Mater. Sci. Technol.* **2013**, *29*, 317–322. https://doi.org/10.1016/j.jmst.2013.02.002
50. R. S. R. Isaac, G. Sakthivel, C. Murthy, *J. Nanotech.* **2013**, *13*, 1–6.
51. M. Ghaffari-Moghaddam, R. Hadi-Dabanlou, *J. Ind. Eng. Chem.* **2014**, *20*, 739–744. https://doi.org/10.1016/j.jiec.2013.09.005
52. P. S. Ramesh, T. Kokila, D. Geetha, *Spectrochim. Acta A* **2015**, *142*, 339–343. https://doi.org/10.1016/j.saa.2015.01.062
53. Y. Gao, Q. Huang, Q. Su, R. Liu, *Spect. Lett*. **2014**, *47*, 790–795. https://doi.org/10.1080/00387010.2013.848898
54. M. Chandrasekaran, A. H. Bahkali, *Saudi J. Biol. Sci.* **2013**, *20*, 105–120. https://doi.org/10.1016/j.sjbs.2012.12.004
55. J. Wang, C. M. Rosell, C. B. Barber, *Food Chem.* **2002**, *79*, 221–226. https://doi.org/10.1016/S0308-8146(02)00135-8
56. A. Paraskevopoulou, D. Boskou, V. Kiosseoglou, *Food Chem.* **2005**, *90*, 627–634. https://doi.org/10.1016/j.foodchem.2004.04.023
57. M. Abdelhak, E. Guendez, K. Eugene, K. Panagiotis, *Food Chem.* **2005**, *89*, 411–420. https://doi.org/10.1016/j.foodchem.2004.02.051
58. P. K. Vayalil, *J. Agric. Food. Chem.* **2002**, *50*, 610–617. https://doi.org/10.1021/jf010716t
59. F. Bilgari, A. F. M. Alkarkhi, A. M. Easa, *Food Chem.* **2008**, *107*, 1636–1641. https://doi.org/10.1016/j.foodchem.2007.10.033
60. M. S. Baliga, B. R. V. Baliga, S. M. Kandathil, H. P. Bhat, P. K. Vayalil, *Food. Res. Int.* **2011**, *44*, 1812–1822. https://doi.org/10.1016/j.foodres.2010.07.004
61. A. M. Fayaz, K. Balaji, P. T. Kalaichelvan, R. Venkatesan, *Colloids Surf. B* **2009**, *74*, 123–126. https://doi.org/10.1016/j.colsurfb.2009.07.002
62. J. Park, J. Joo, S. G. Kwon, Y. Jang, T. Hyeon, *Angew. Chem. Inter. Ed.* **2007**, *46*, 4630–4660.
63. S. M. Roopan, G. Madhumitha, A. A. Rahuman, C. Kamaraj, A. Bharathi, T. V. Surendra, *Ind. Crop. Prod.* **2013**, *43*, 631–635. https://doi.org/10.1016/j.indcrop.2012.08.013
64. H. M. M. Ibrahim, *J. Rad. Res. Appl. Sci.* **2015**, *8*, 265–275.
65. D. A. Kumar, V. Palanichamy, S. M. Roopan, *Spectrochim. Acta A* **2014**, *127*, 168–171. https://doi.org/10.1016/j.saa.2014.02.058
66. R. Kumar, S. M. Roopan, A. Prabhakarn, V. G. Khanna, S. Chakroborty, *Spectrochim. Acta A* **2012**, *90*, 173–176. https://doi.org/10.1016/j.saa.2012.01.029
67. S. Naraginti, A. Sivakumar, *Spectrochim. Acta A* **2014**, *128*, 357–362. https://doi.org/10.1016/j.saa.2014.02.083
68. M. Nasrollahzadeh, S. M. Sajadi, A. Rostami-Vartooni, M. Khalaj, *J. Mol. Catal. A: Chem.* **2015**, *396,* 31–39.

https://doi.org/10.1016/j.molcata.2014.09.029
69. M. Nasrollahzadeh, S. M. Sajadi, A. Rostami-Vartooni, M. Alizadeh, M. Bagherzadeh *J. Colloid Interface Sci.* **2016**, *466*, 360–368. https://doi.org/10.1016/j.jcis.2015.12.036
70. A. Rostami-Vartooni, M. Nasrollahzadeh, M. Salavati-Niasari, M. Atarod, *J. Alloys Compd.* **2016**, *689*, 15–20. https://doi.org/10.1016/j.jallcom.2016.07.253
71. R. J. Kalbasi, A. A. Nourbakhsh, F. Babaknezhad, *Catal. Commun.* **2011**, *12*, 955–960. https://doi.org/10.1016/j.catcom.2011.02.019
72. S. Y. Gao, X. X. Jia, Z. D. Li, Y. L. Chen, *J. Nanopart. Res.* **2012**, *14*, 1–11.
73. Z. Duan, G. Ma, W. Zhang, *Bull. Korean Chem. Soc.* **2012**, *33*, 4003–4006. https://doi.org/10.5012/bkcs.2012.33.12.4003
74. A. K. Shil, D. Sharma, N. R. Guha, P. Das, *Tetrahedron Lett*. **2012**, *53*, 4858–4861. https://doi.org/10.1016/j.tetlet.2012.06.132
75. Y. Choi, H. S. Bae, E. Seo, S. Jang, K. H. Park, B. S. Kim, *J. Mater. Chem.* **2011**, *21*, 15431–15436. https://doi.org/10.1039/c1jm12477c
76. M. Nasrollahzadeh, M. Bagherzadeh, H. Karimi, *J. Colloid Interface Sci.* **2016**, 465, 271–278. https://doi.org/10.1016/j.jcis.2015.11.074
77. K. L. Wu, R. Yu, X. W. Wei, *Cryst. Eng. Commun.* **2012**, *14*, 7626–7632. https://doi.org/10.1039/c2ce25457c
78. K. L. Wu, X. W. Wei, X. M. Zhou, D. H. Wu, X. W. Liu, Y. Ye, Q. Wang, *J. Phys. Chem. C* **201**1, *115*, 16268–16274. https://doi.org/10.1021/jp201660w
79. S. Liu, Z. Chen, N. Zhang, Z. R. Tang, Y. J. Xu, *J. Phys. Chem. C*, **2013**, *117*, 8251–8261. https://doi.org/10.1021/jp400550t
80. W. Che, Y. Ni, Y. Zhang, Y. Ma, *J. Phys. Chem. Solids* **2015**, *77*, 1–7. https://doi.org/10.1016/j.jpcs.2014.09.006
81. D. Z. Jiang, J. Xie, D. Jiang, X. Wei, M. Chen, *Cryst. Eng. Comm.* **2013**, *15*, 560–569. https://doi.org/10.1039/C2CE26398J
82. J. Feng, L. Su, Y. Ma, C. Ren, Q. Guo, X. Chen, *Chem. Eng. J.* **2013**, *221*,16–24. https://doi.org/10.1016/j.cej.2013.02.009
83. Q. Cui, B. Xia, S. Mitzscherling, A. Masic, L. Li, M. Bargheer, H. Möhwald, *Colloids Surf. A: Physicochem. Eng. Aspects* **2015**, *465*, 20–25. https://doi.org/10.1016/j.colsurfa.2014.10.028
84. M. Atarod, M. Nasrollahzadeh, S. M. Sajadi, *J. Colloid Interface Sci.* **2016,** *465,* 249–258 https://doi.org/10.1016/j.jcis.2015.11.060
85. M. Nasrollahzadeh, M. Atarod, S. M. Sajadi, *Appl. Surf. Sci.* **2016**, *364*, 636–644. https://doi.org/10.1016/j.apsusc.2015.12.209
86. M. Nasrollahzadeh, S. M. Sajadi, *Ceram. Int.* **2015**, *41*, 14435–14439. https://doi.org/10.1016/j.ceramint.2015.07.079

Povzetek

V tem članku poročamo o sintezi sferičnih nanodelcev srebra (Ag NPs), ki smo jih sintetizirali s poceni, hitrim, enostavnim in okolju prijaznim pristopom. Za sintezo smo uporabili sadni izvleček datljeve palme kot naraven reducent in stabilizator. Produkte smo karakterizirali z UV-Vis spektroskopijo, rentgensko praškovno difrakcijo (XRD), infrardečo spektroskopijo (FT-IR), vrstično elektronsko mikroskopijo (FE-SEM), presevno elektronsko mikroskopijo (TEM), mikroskopijo na atomsko silo (AFM), energijsko disperzivno rentgensko spektroskopija (EDX) in meritvami zeta potenciala. Preučevali smo različne parametre reakcijskih pogojev kot so čas, množine reducenta in srebrovega nitrata, temperatura, pH. Optimalni reakcijski pogoji sinteze srebrovih nanodelcev (Ag NPs) so bili doseženi v primeru reakcije 10 mM raztopine srebrovega nitrata s sadnim izvlečkom datljeve palme pri pH 11 in temperaturi do 55 ° C v 10 minutah. Elementarno in kristalinično naravo nanodelcev srebra (Ag NPS) smo potrdili z EDX in XRD analizama. SEM in TEM slike so pokazale, da so nanodelci srebra (Ag NPs) sferični, z velikostjo v območju od 25-60 nm. Na osnovi FT-IR analize, lahko rečemo, da so funkcionalne skupine prisotne v bioloških molekulah sadnega izvlečka datljevih palm odgovorne za redukcijo in stabilizacijo nanodelcev srebra (Ag NPs). Dokazali smo njihovo učinkovito antibakterijsko delovanje proti nekaterim patogenim bakterijam. Preučevali smo tudi katalitsko aktivnost nanodelcev srebra (Ag NPs) za hitro in učinkovito zmanjšanje strupenih nitro spojin v manj strupene amine z uporabo $NaBH_4$